

The present-day thermal and chemical structure with Vs profiles predicted from the lunar overturn model.

N. Zhang, E. M. Parmentier, Y. Liang, Department of Geological Science, Brown University, 02912, RI. (Nan_zhang@brown.edu)

Introduction: Standard lunar evolution models involve giant impact, lunar magma ocean, and cumulate overturn. One potential outcome of lunar cumulate mantle overturn is the presence of ilmenite-bearing cumulates (IBC) at the base of the lunar mantle. Because the dense IBC layer is enriched in heat producing elements, it may become thermally buoyant with respect to the overlying cumulate harzburgitic mantle at a later time. Upwelling of the ilmenite-bearing cumulate layer has been used to explain the genesis of mare basalts.

Another important constraint for the lunar evolution is the present-day deep mantle structures (see Fig. 1C). The Apollo seismic experiment recorded deep moonquakes located from 600 to 1000 km depth [1]. They appear to originate from repeatedly activated nests located on the Moon's nearside hemisphere [2]. Seismic arrivals along ray paths that pass through 1000 km depth are not detected, which suggests mantle in this region is highly attenuating, possibly partially molten [3]. These seismic data have been used to invert the density, V_p , and V_s profiles [4,5]. Weber et al. (2011) proposed the presence of a 150 km layer of extremely low seismic velocities on the core-mantle boundary (CMB).

This study focuses on the present-day mantle structures. We compare the seismically inferred structures with those predicted by 3-D overturn models [6]. Specifically, we use our temperature and chemical fields to calculate V_s profiles that are compared to the seismically inverted V_s profiles. The effect of the Mg# stratification on the V_s profile is also investigated.

Model: The basic model formulation can be found in [6]. Here, we emphasize the KREEP distribution and the laboratory-derived, temperature-dependent rheology. We adopt parameters consistent with observed viscosity of the Earth's upper mantle with an activation energy of 200 kJ/mol. Reference viscosities at 1300°C are 5×10^{18} and 1×10^{21} Pa.s for wet and dry harzburgite mantle, respectively [7]. 20%, 50%, or 100% of total KREEP has been distributed in the IBC layer on the CMB. The mantle cumulate layer beneath the crust maintains the remaining part. For the V_s calculation, the temperature and pressure dependence of the density is calibrated with the 3rd order Birch-Murnaghan EOS. Most of the material properties are based on the table from [8]. The material properties for the ilmenite are taken from [9].

Predicted 3-D mantle structures and 1-D temperature and chemical profiles: Figure 1A and B show a 3-D simulation in which the IBC layer contains 20%

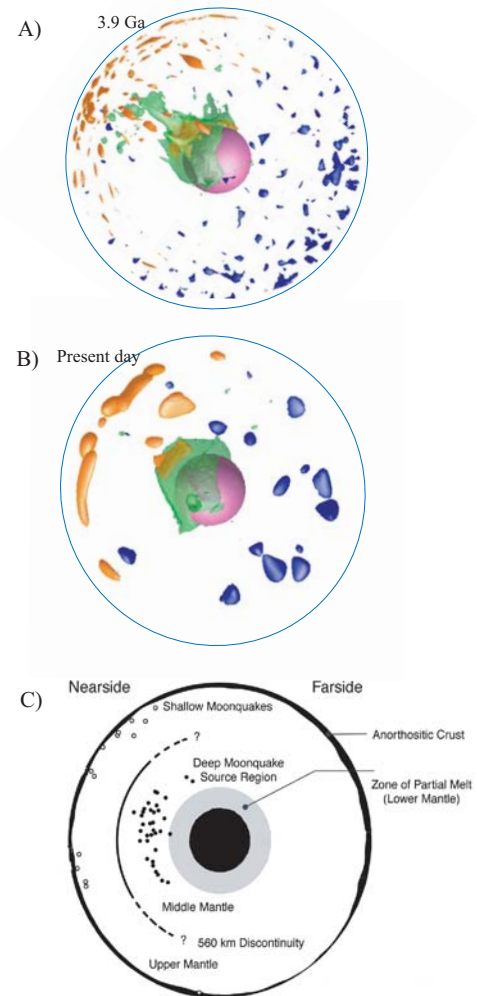


Figure 1. The calculated (A and B) and observed (C) (modified from Wieczorec 2009) mantle structures. The observed deep moonquakes (C) may be related to IBC piles (B) left by the single IBC plume.

KREEP and the reference viscosity uses 5×10^{18} Pa.s. The results show a single chemical plume at 3.9 Ga (Fig. 1A), which provides a mechanism for the asymmetrical distribution of Mare basalts on the lunar surface. This case also shows an IBC pile on the CMB of the nearside at the present day (Fig. 1B), which may explain the observed deep moonquakes (Fig. 1C).

The present-day temperature and chemical profiles (spherically averaged) are shown in Fig. 2. Basically, our models show that a wet lunar mantle ($\eta_{\text{ref}}=5 \times 10^{18}$ Pa.s) can lose heat fast and cause a cool lunar mantle (Fig. 1A). More KREEP in the deep IBC layer results in hotter mantle (Fig. 1A; green, blue, and black curves). The chemical profiles show that only part of the IBC has risen or been entrained to the upper mantle (Fig. 2B). Overall, a layer with high IBC concentration remains on the CMB to the present day.

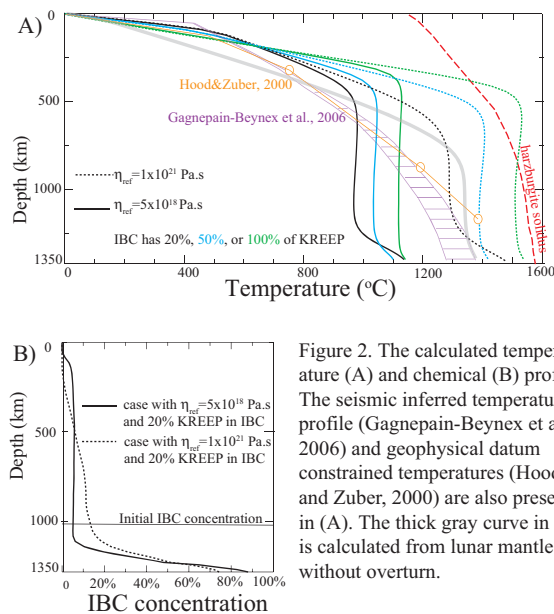


Figure 2. The calculated temperature (A) and chemical (B) profiles. The seismic inferred temperature profile (Gagnepain-Beynax et al., 2006) and geophysical datum constrained temperatures (Hood and Zuber, 2000) are also presented in (A). The thick gray curve in (A) is calculated from lunar mantle without overturn.

The calculations of Vs profiles: The calculation of the Vs profile involves three steps. In the first step, we use the 3rd Birch-Murnaghan EOS and our predicted temperature profile to calculate the density profile. The resultant density only increases slightly with depth due to relatively slow increase of pressure with depth. This is consistent with previous studies [e.g., 4, 10]. The second step involves the mineralogical model and bulk Mg#. We refer to Snyder's model [11] for lunar mantle solidification and assume 52% olivine and 48% opx for the lunar mantle. As an example, we use $\text{Mg\#} = 80$ for the bulk Moon [12]. With these assumptions, we obtain the Vs profile as shown in Fig. 3A (yellow curve). Although this Vs profile is generally consistent with the profiles from the seismic inversions in the upper mantle, it shows a large difference to the Vs profile around the CMB (Fig. 3A, green curve). In the last step, we have to understand how the overturn model changes the depth dependence of the Mg#. We start from the Mg# profile before the overturn (Fig. 3B, dashed gray curve) [11]. After overturn, the Mg# changes to profile shown with dashed black curve in Fig. 3B. Because at the beginning of model evolution, the IBC layer has separated convection from above mantle convection, the Mg# is homogenized in these two separate layers (Fig. 3B, blue curve). Finally, following the IBC evolution (Fig. 2B), the Mg# evolves

to a profile showing a significant increase on the CMB (Fig. 3B, purple curve). With this Mg# profile, we obtain a Vs profile shown as the purple curve in Fig. 3A.

Comparison with uniform composition models:

We also generated models with uniform composition, similar to [13,14]. The temperature and Vs profiles are shown as thick gray curve in Fig. 2A and black curve in Fig. 3A. In the absence of chemical stratification, the Vs profile shows no low velocity layer on the CMB.

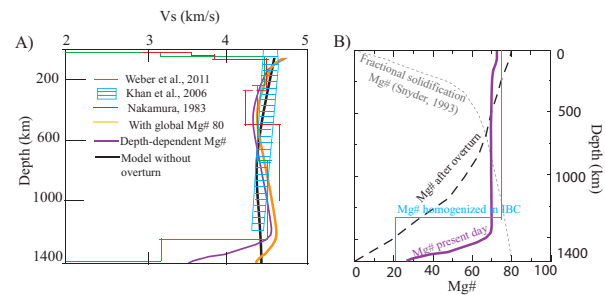


Figure 3. the seismic inverted and calculated Vs profiles (A), and the evolution of Mg# with our overturn model (B).

Discussion and Conclusions: Weber et al. (2011) have argued that the low Vs velocity on the CMB is caused by the partial melt. For the overturn model, one difficulty is how to prevent the dense ilmenite-rich melt segregating downwards. With reasonable parameters for the ilmenite-rich melt and IBC solid matrix, we estimate the segregation time as 15 Ma, much shorter than the mantle cooling time (~100 Ma). Alternatively, can models without chemical stratification due to overturn produce a partial melt layer on the CMB? The answer is negative. These models without overturn start from the mantle solidus, always cool with time, and are not able to produce temperature higher than solidus on the CMB. This suggests that the presence of Vs reduction on the CMB is a consequence of chemical stratification due to mantle overturn.

References: [1] M. Wieczorek (2009) *Elements* 5, 35-40. [2] Y. Nakamura, (2003) *Physics of the Earth and Planetary Interiors*, 139, 197-205. [3] Y. Nakamura, (2005) *J. Geophys. Res.* 110, 2015-1030. [4] A. Khan, MacLennan J., S. Taylor, and Connolly J., (2006) *J. Geophys. Res.*, 111, 131-140. [5] R. Weber, Lin P.-Y., Garnero E., Williams Q., and Lognonne P. (2011) *Science*, 331, 309-312. [6] N. Zhang, EM. Parmentier, and Liang Y. (2012) *LPS XXXIX*, abstract # 2641. [7] G. Hirth and Kohlstedt D. (1996) *Earth Planet. Sci. Lett.*, 292, 139-147. [8] L. Stixrude and C. Lithgow-Bertelloni, (2005) *Geophys. J. Inter.*, 162, 610-632. [9] E. Tronche, van Parker M. et al., (2010) *American Mineral.* 95, 1708-1716. [10] F. Nimmo, Faul U., and Garnero E., (2012) *J. Geophys. Res.*, 117, 1413-1454. [11] G. Snyder, et al., (1992) *Geochim. Cosmochim. Acta* 56, 3809-3823. [12] S. Taylor et al., (2006) *GCA*, 70, 5904-5918. [13] T. Spohn, et al., (2001) *Icarus*, 149, 54-65. [14] Toksoz et al., (1978) *The Moon and Planets* 18: 281-320.